Biochimica et Biophysica Acta, 1112 (1992) 67–74
© 1992 Elsevier Science Publishers B.V. All rights reserved 0005-2736/92/$05.00

BBAMEM 75812

Single Ca^{2+}-activated K^+ channels in human erythrocytes: Ca^{2+} dependence of opening frequency but not of open lifetimes

Trese Leinders, Regina G.D.M. van Kleef and Henk P.M. Vijverberg

Research Institute of Toxicology, University of Utrecht, Utrecht (Netherlands)

(Received 18 May 1992)

Key words: Calcium ion-activated potassium ion channel; Potassium ion channel; Single-channel patch clamp; Patch clamp; Calcium ion dependence; Voltage dependence; Erythrocyte; (Human)

Using the patch-clamp technique single-channel properties of Ca^{2+}-activated K^+ (CaK) channels were investigated in inside-out membrane patches of human erythrocytes. In a physiological K^+ gradient (5 mM K^+ externally; 150 mM K^+ internally) the single CaK channel conductance is 15 pS in the membrane potential range of −40 to +40 mV. The channel open probability, opening frequency and open and closed time distributions are voltage-independent. The open probability and the opening frequency of the CaK channel depend on $[Ca^{2+}]_i$ and increase between 0.5 and 60 μM Ca^{2+} from approx. 10% to 90% of the maximum value obtained at 115 μM. The relation between open probability and $[Ca^{2+}]_i$ can be described by a sigmoid concentration-effect curve with an EC_{50} of 4.7 μM and a slope factor of 1. Independent of $[Ca^{2+}]_i$ open time distributions yield two time constants of 5.3 and 22 ms. The relative amplitudes of the fast and slow components of the open time histogram as well as the maximum open probability and the maximum opening frequency of CaK channels vary considerably. In addition, CaK channels in multiple channel patches are highly interdependent. It is concluded that the Ca^{2+}-dependence of CaK channels in human erythrocytes is due to the modulation of opening frequency by internal Ca^{2+}. The results are consistent with a classical receptor-agonist model in which ligand interaction kinetics are much faster than channel gating.

Introduction

A causal relation between elevation of the internal calcium concentration, $[Ca^{2+}]_i$, and an increase in the K^+ permeability was initially found in human erythrocytes treated with glycolytic inhibitors [1]. In ion flux studies the site at which Ca^{2+} enhances K^+ permeability has been localized at the inner membrane surface. Half-maximum responses of K^+ efflux have been obtained at 0.3–3.0 μM Ca^{2+} [2–5]. The enhancement of K^+ efflux is blocked by tetraethylammonium (TEA) ions [6], by charybdotoxin [5] and by quinine, whereas apamin has no effect at either side of the erythrocyte ghost membrane [7]. In addition, variation of cellular ion concentrations has demonstrated that the Ca^{2+}-dependent K^+ flux is blocked by internal Na^+ [2,3].

Application of the patch clamp technique has shown that the Ca^{2+}-evoked increase in erythrocyte K^+ permeability is due to the opening of Ca^{2+}-activated K^+ (CaK) channels with a single-channel conductance of 10–40 pS in symmetric high K^+ solutions [8–10]. CaK channels in human erythrocytes are blocked by quinine and by Na^+ at either side of the membrane, by external TEA and by internal Mg^{2+} [11,12]. TEA and external Na^+ reduce the single-channel conductance, whereas internal quinine and Mg^{2+} reduce the open probability [11]. Except for the pharmacology of the CaK channel in human erythrocytes, the Ca^{2+}-dependence of the CaK channel has only been investigated in symmetric high K^+ solutions at the very negative holding potential of −100 mV [9–11,13]. Under these conditions increasing $[Ca^{2+}]_i$ enhances the open probability of CaK channels. At 20°C half-maximum open probability is attained at 2 μM Ca^{2+} [10]. Both the mean open time and the mean closed time were reported to depend on $[Ca^{2+}]_i$ and it has been suggested that two Ca^{2+} ions are required for channel opening [9]. Depending on temperature, one to two open states and two closed states of the CaK channel were found [13]. It has been mentioned that the opening frequency of CaK channels in human erythrocytes is not voltage-dependent and that these channels do not inactivate [8].

The present study reports on the mechanism of operation of the CaK channel in inside-out patches of human erythrocytes using more physiological condi-

Correspondence to: H.P.M. Vijverberg, Research Institute of Toxicology, University of Utrecht, P.O. Box 80176, 3508 TD Utrecht, Netherlands.

tions. The Ca^{2+}-dependent mechanism of operation of these channels is investigated by separation of the single-channel parameters that determine open probability at various well-defined $[Ca^{2+}]_i$. A part of the results has been published in abstract form [14].

Materials and Methods

Experimental procedure. Erythrocytes were obtained from healthy donors by fingertip puncture and were used at the same day. A drop of blood was immediately diluted in 0.5 ml of external solution (see below) in an Eppendorf tube and stored at 4°C. Aliquots of the diluted sample were once more diluted in a tissue culture dish to obtain a low density of blood cells loosely attached to the bottom of the dish. For patch clamp experiments the culture dish was placed on the stage of an inverted phase-contrast microscope. Erythrocytes were selected by their characteristic shape at a magnification of 300 ×.

Single CaK channel currents were recorded as described by Hamill et al. [15]. Fire-polished borosilicate glass pipettes (Clark GC150) with a resistance of 10–40 MΩ were used. After formation of a gigaseal (16–53 GΩ) the attached cell was broken by making it touch the bottom of the culture dish. Generally, this procedure left the inside-out patch and the gigaseal intact. The holding potential was 0 mV, unless otherwise stated. Patches were superfused with control and test solutions (see below) using two pipettes (diameter 100 μm) at a flow rate of 350–400 μl/min. The opening of the superfusing pipette was always within 50 μm of the patch. Experiments were performed at a room temperature of 20–24°C.

Single-channel currents were low-pass filtered using an 8 pole Bessel filter (−3 dB at 300 Hz) and digitized (8 bits; 0.5 ms sample interval; 1024 points/record). For each $[Ca^{2+}]_i$ at least 100 records, i.e., 50 s of steady-state channel activity, were stored on magnetic disc for off-line analysis.

Data analysis and statistics. Data were obtained by superfusion of inside-out patches with the various test solutions in a semi-random order alternated by superfusion with control internal solution. The patches were repeatedly superfused with internal solution containing a saturating $[Ca^{2+}]$. Patches with trends in the open probability of channels or a maximum open probability < 0.10 were excluded from further analysis. Transitions between open and closed states were detected using a half-amplitude threshold criterion and a minimum event width of 2.5 ms. The number of channels (N_c) in each patch was estimated as the maximum number of channels simultaneously open under conditions of maximum open probability. Open probability (P_O) was determined by dividing the sum of all open times by the total observation time. Note that for independent ion channels P_O should be proportional to N_c and that $0 \leq P_O \leq N_c$. The frequency of channel opening was determined as the ratio between the number of opening transitions and the total observation time.

Events were divided into classes of approximately equal frequency and presented as frequency density histograms [16]. Exponential time constants were estimated by minimizing χ^2 using a Levenberg-Marquardt nonlinear least-squares algorithm [17]. Dual exponential fitting was performed only when a single-exponential distribution was rejected by the χ^2 goodness-of-fit test ($\alpha = 0.05$). Open time frequency density histograms were constructed from single open events only. Results of multiple channel patches did not deviate from those of apparent single-channel patches.

Concentration-effect curves were fitted by minimizing the sum of squared deviations from the mass-action law equation:

$$E = \frac{E_{max}}{(1 + \{EC_{50}/[Ca^{2+}]\}^n)} \quad (1)$$

by the Levenberg-Marquardt algorithm.

Linearity and regression tests were performed by least-squares regression analysis [18]. Results are presented as means ± calculated or, in case of curve fitting, estimated S.D., unless otherwise stated.

Solutions and chemicals. All solutions were prepared from milli-Q/UF purified water (Millipore, Bedford, USA). External solution contained (mM): NaCl, 145; KCl, 5; Hepes, 20; $CaCl_2$, 1.8; and $MgCl_2$, 0.8. The pH was adjusted to 7.4 with approximately 8.4 mM NaOH and the osmolarity was adjusted to 330 mosmol/l with 30 mM glucose. The internal solution for inside-out patches contained (mM): KNO_3, 120; Hepes, 10; Ca^{2+} buffer (citric acid, EGTA or nitrilotriacetic acid), 10; and variable concentration of $Ca(NO_3)_2$. The pH was adjusted to 7.2 with approximately 30 mM KOH and the osmolarity was adjusted to 300 mosmol/l with 55 mM sucrose. In some experiments nitrilotriacetic acid (NTA) and ethyleneglycol bis(β-aminoethyl ether)-*N*,*N*'-tetraacetic acid (EGTA) were used instead of citric acid to verify that the Ca^{2+} buffer was without effect. No Na^+ was added to the internal solution to avoid channel block [2,3,12]. Because heavy metals may affect Ca^{2+}-activated K^+ channels [19,20], ultrapure chemicals were used to prepare the internal solution. The final maximum concentration of contaminants, calculated from the data supplied with the chemicals, was (μM): Ba, 1.1; Ca, 1.8; Cd, 0.11; Co, 0.20; Mg, 0.57; Na, 7.6; and Pb, 0.075. Ca^{2+} buffer compositions were calculated [21] using stability constants from Sillen and Martell [22]. Free $[Ca^{2+}]$ of the various solutions was also measured by the fura-2 method and using a Ca^{2+}-selective electrode. Control internal solution con-

tained < 10 nM free Ca^{2+}. In the range < 0.5 μM and ≥ 10 μM Ca^{2+} deviations were ≤ 3%, whereas at 1 μM Ca^{2+} a deviation of 30% was observed. The latter deviation is most likely due to the fact that in the micromolar range buffers of EGTA and citrate are relatively weak and the fura-2 as well as the Ca^{2+}-electrode method are least accurate. Calculated values are indicated throughout.

KNO_3 (Suprapure), $Ca(NO_3)_2$ (Suprapure) were obtained from Alfa Products, Karlsruhe, Germany; NaCl (pro analysi) and KCl (pro analysi), KOH (Ultrapure) from Merck, Darmstadt, Germany; Hepes (Micro-Select) from Fluka, Buchs, Switzerland; $CaCl_2$ (AnalR), citric acid (AnalR), sucrose (Aristar) and glucose (Aristar) from BDH, Poole, UK; $MgCl_2$ (Baker Analysed reagent) from J.T. Baker, Deventer, Netherlands; EGTA from Sigma, St. Louis, USA.

Results

Alternate superfusion of inside-out membrane patches of human erythrocytes with control and Ca^{2+}-containing internal solution revealed three types of Ca^{2+}-activated channels. Two of these channels carried outward currents of 0.3 pA and 0.9 pA at the holding potential of 0 mV. An additional channel with a reversal potential near 0 mV became apparent at non-zero holding potentials. The latter type of channel and the 0.3 pA channel were infrequently observed and will be ignored. Data presented were obtained from patches in which these channels were absent.

The single CaK channel conductance was calculated from *I–V* relationships of unitary currents obtained from inside-out membrane patches during superfusion with internal solution containing 3.6 μM or 115 μM Ca^{2+} at holding potentials between −60 and +40 mV (Fig. 1). The *I–V* relationship is consistent with the notion that the current through the CaK channel is mainly carried by K^+ and rectification is observed in the potential range more negative than −40 mV. *I–V* relationships obtained from three patches at 3.6 and 115 μM Ca^{2+} were found to be Ca^{2+}-independent ($P = 0.79$–0.95). Regression analysis on the channel amplitudes of four patches showed that in the range of −40 to +40 mV none of the *I–V* relationships differs from linear statistically ($P = 0.13$–0.58) and that they are identical ($P = 0.06$–0.91). The mean single-channel conductance amounted to 15 ± 0.5 pS ($n = 4$).

Ca^{2+} dependence

Sets of consecutive traces and amplitude histograms of CaK channel activity at various $[Ca^{2+}]_i$ are shown in Fig. 2. Both single-channel records and amplitude histograms demonstrate that the open probability (P_O) increases with increasing $[Ca^{2+}]_i$. Fig. 3a shows the relation between the P_O and free $[Ca^{2+}]_i$ of four

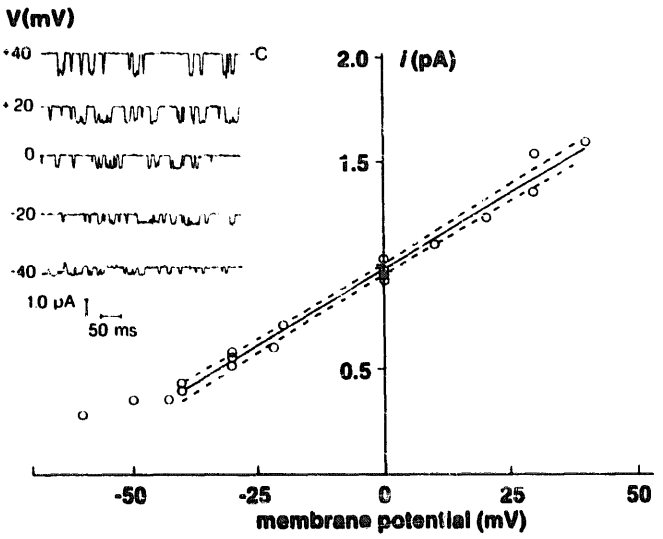

Fig. 1. Amplitude of the unitary currents through a single Ca^{2+}-activated K^+ channel of a human erythrocyte recorded at various membrane potentials. The solid line represents the least-squares regression of the *I–V* relationship between −40 and +40 mV measured at 115 μM Ca^{2+} yielding a single-channel conductance of 14.5 ± 1.0 pS (95% confidence limit; dotted line). No significant deviation from linearity was observed ($P = 0.53$). The inset shows traces of the single Ca^{2+}-activated K^+ channel recorded at various membrane potentials. The closed level is marked C.

patches. The P_O values of individual patches were normalized to the value obtained at 115 μM Ca^{2+}. The concentration-effect curve is the mean of the individual curves fitted according to Eqn. 1 to the data obtained at eight different $[Ca^{2+}]_i$ from each patch. Between 0.5 and 60 μM Ca^{2+} the P_O increases from 10 to 90% of its maximum value. The mean EC_{50} value is 4.7 ± 0.2 μM and the mean slope factor 0.98 ± 0.08 (Table 1). Data from six other patches, in which only four different $[Ca^{2+}]_i$ were tested, have been fitted according to Eqn. 1 with a slope factor fixed to 1 and yielded a mean EC_{50} of 4.9 ± 2.4 μM.

The fraction of time a channel spends in the open state is determined by its opening frequency as well as by the lifetime of the open state. Fig. 3b shows that the opening frequency increases with increasing $[Ca^{2+}]_i$. The fitted line represents the mean concentration-effect curve obtained from the same patches used in Fig. 3a. The mean EC_{50} value was calculated to be 4.3 ± 0.8 μM and the mean slope factor 0.82 ± 0.13 (Table 1). Data from the other six patches, obtained at four different $[Ca^{2+}]_i$, yielded a mean EC_{50} of 3.7 ± 2.2 μM using a slope factor fixed to 1.

One of the patches was also superfused with internal solutions in which citric acid was replaced by NTA to buffer $[Ca^{2+}]_i$ at 1 and 10 μM or by EGTA to buffer $[Ca^{2+}]_i$ at 0.5 μM. The open probability and the opening frequency appeared to depend only on $[Ca^{2+}]_i$ and not on the Ca^{2+} buffer used (see Fig. 3a,b).

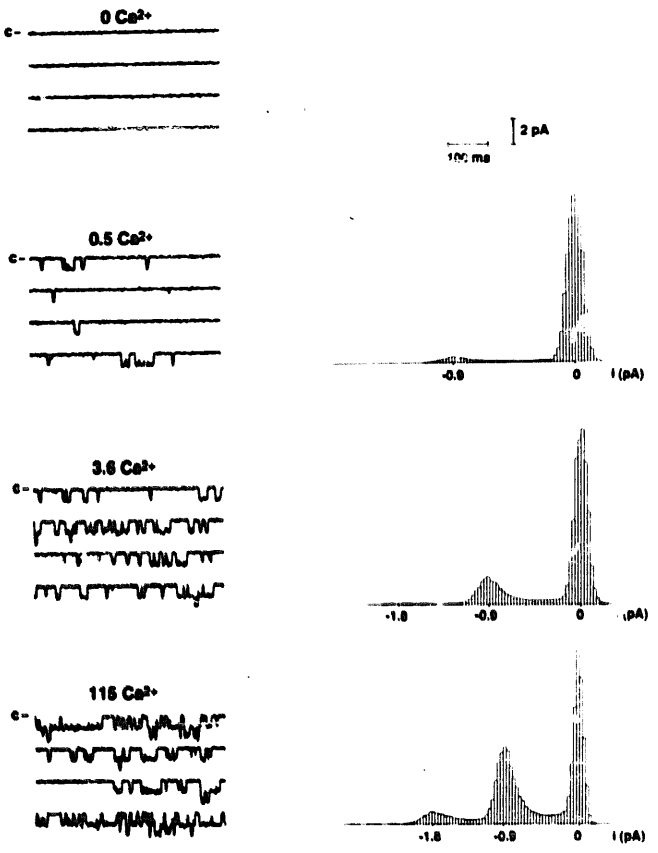

Fig. 2. A Ca^{2+}-activated K^+ channel recorded at 0 mV in an inside-out patch of human erythrocyte. The left panel shows sets of consecutive traces of events recorded at various $[Ca^{2+}]_i$. All records have been obtained from the same patch. The right panel shows the corresponding amplitude histograms of the complete data obtained at the free Ca^{2+} concentration indicated in μM. The closed level is marked C.

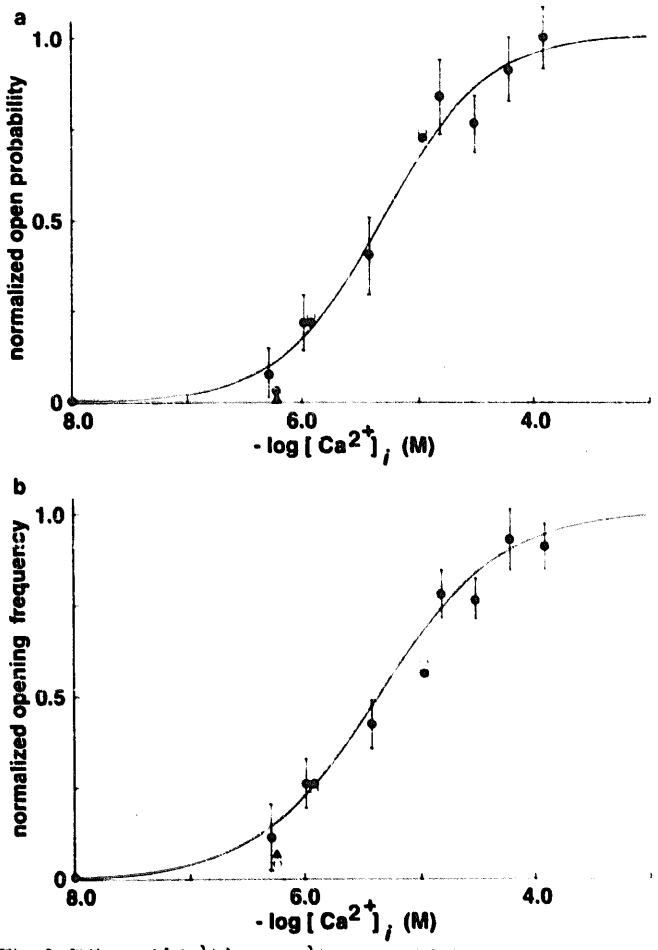

Fig. 3. Effect of $[Ca^{2+}]_i$ on Ca^{2+}-activated K^+ channels of human erythrocytes in inside-out membrane patches at 0 mV membrane potential. Datapoints with bars are mean ± S.D. of four patches. (a) the Ca^{2+} dependence of the normalized open probability was fitted by a concentration-effect curve with an EC_{50} value = 4.7 ± 0.2 μM and a slope factor = 0.96 + 0.09. (b) the Ca^{2+} dependence of the normalized opening frequency was fitted by a concentration-effect curve with an EC_{50} value = 4.3 ± 0.9 μM and slope factor = 0.77 ± 0.09. In one patch citric acid (●) and NTA (○) were used to buffer $[Ca^{2+}]_i$ at 1 and 10 μM, and citric acid as well as EGTA (▲) were used to buffer $[Ca^{2+}]_i$ at 0.5 μM. Datapoints obtained from these measurements are given without bars and have not been used for fitting.

The maximum open probability and the maximum opening frequency were disproportional to the maximum number of channels (N_c) observed in the patch, indicating that either N_c was underestimated or channels in different patches behave differently (Table I). Analysis of the probabilities of finding multiple open levels revealed that the channels do not behave independently. In patch ery0725 the probabilities of exactly 0, 1, 2, 3 and 4 channels open at 115 μM Ca^{2+} amounted to 0.25, 0.52, 0.20, 0.018 and 0.0002, respectively. The probabilities of multiple open channels are much smaller than expected from the binomial distribution. A similar deviation from independent behaviour was generally observed in other patches as well as at non-saturating $[Ca^{2+}]_i$.

Open time frequency density distributions obtained at seven different $[Ca^{2+}]_i$ values between 1.0 and 115 μM in three patches were fitted by the sum of two exponential functions (Fig. 4a,b). No dependence on $[Ca^{2+}]_i$ ($P = 0.28$–0.98) was found for the two open time constants (Fig. 4c). The mean open time constants of 12 patches were 5.3 ± 2.3 ms and 22 ± 9 ms. The

TABLE I

Ca^{2+} dependence of the open probability and the opening frequency of human erythrocyte CaK channels

N_c is the maximum number of channels that have been observed in the open state simultaneously under conditions of $P_{O,max}$.

Patch	N_c	Open probability			Opening frequency		
		EC_{50} (μM)	slope	E_{max}	EC_{50} (μM)	slope	E_{max} (Hz)
ery0918	1	4.5	1.05	0.16	3.4	0.66	26.64
ery0921	2	4.9	0.97	0.14	5.3	0.85	32.14
ery0711	3	4.6	1.04	0.77	4.1	0.98	46.16
ery0725	4	4.7	0.87	0.98	4.3	0.81	67.47

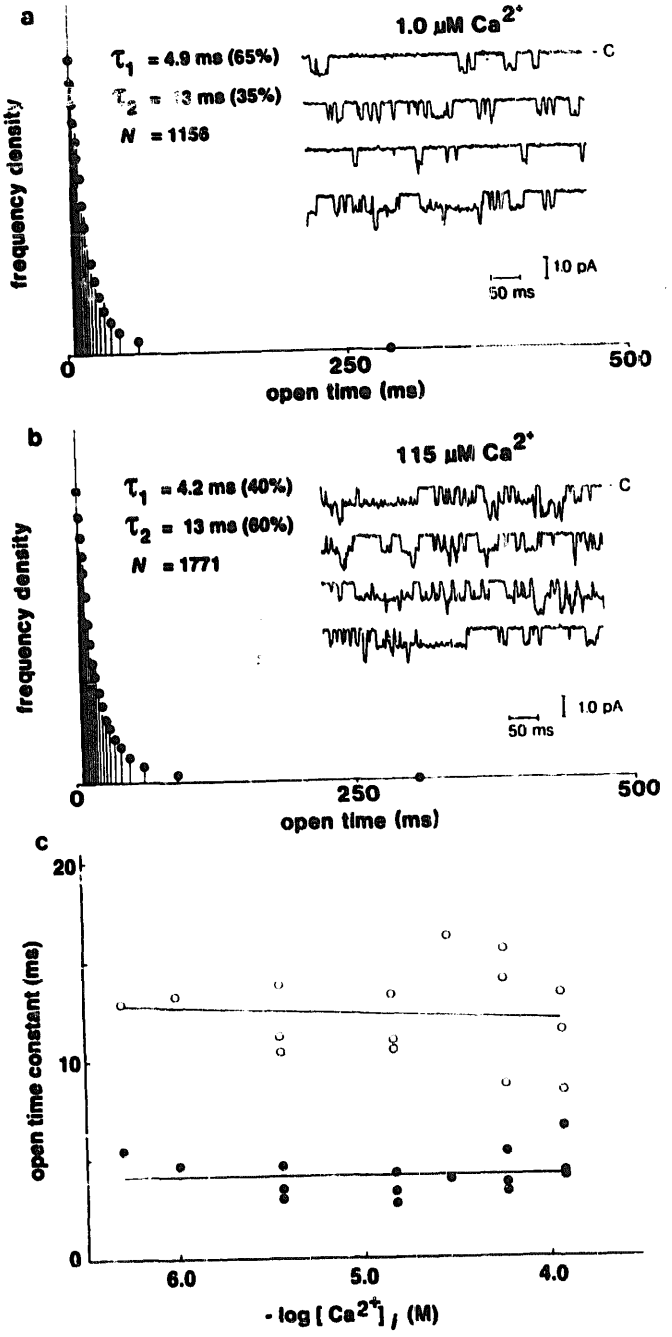

Fig. 4. Effect of $[Ca^{2+}]_i$ on the Ca^{2+}-activated K^+ channel open time distributions of human erythrocytes obtained at 0 mV membrane potential. (a), (b) Open time frequency density histograms of patch ery0725 at $[Ca^{2+}]_i$ of 1.0 μM (a) and 115 μM (b) were fitted by the sum of two exponentials. Bars and dots in the frequency density histograms represent measured and fitted values, respectively. Fitted mean time constants (fractional amplitude) and the number of events observed (N) are given in the histograms. The χ^2 (degrees of freedom) and the P values were 22.2 (25) and 0.63 at 1.0 μM Ca^{2+}, and 36.8 (28) and 0.12 at 115 μM Ca^{2+}. Single-exponential fits of these histograms were rejected by the χ^2 goodness-of-fit test at the $P < 0.01$ level. Characteristic consecutive single-channel traces are shown in the inset. The closed level is marked C. (c) The fast and slow open time constants obtained from frequency density histograms of three patches are independent of $[Ca^{2+}]_i$ (no regression: $P = 0.28$ and 0.98, respectively).

relative amplitudes of the fast and the slow component of the open time frequency density histograms varied considerably between patches and also between different sets of data obtained from the same patch. Table II shows that in some patches the amplitudes of the fast and the slow component remained relatively stable, as inferred from the small standard deviation obtained from different sets of data. From these patches it appears that the amplitude ratio varied roughly between 1:4 and 4:1. The large variation in amplitudes of the two exponential components of the open time histograms precludes conclusions with respect to their Ca^{2+} dependence. However, in the careful analysis of all available data overt dependence on any of the experimental conditions or on the blood donors was not apparent.

Closed time frequency density distributions of apparent single-channel patches were adequately fitted by the sum of two exponential functions. For the two closed time constants as well as for the amplitudes of the two fitted exponentials no dependence on $[Ca^{2+}]_i$ was found at six different $[Ca^{2+}]_i$ in the range of 1.0–115 μM ($P = 0.44$–0.74). The mean closed time constants of five apparent single-channel patches were 7.9 ± 3.7 ms and 58 ± 16 ms. The relative amplitudes of the fast and the slow component of closed time frequency density histograms were $42 \pm 12\%$ and $58 \pm 12\%$. The independence of closed time constants and amplitudes of $[Ca^{2+}]_i$ seems to contrast with the finding that the opening frequency is Ca^{2+}-dependent. However, the number of traces without channel opening decreased with increasing $[Ca^{2+}]_i$, indicating the presence of a long-lived closed state. The fraction of the traces without channel opening decreased from 90–100% at 0.5 μM to approx. 1% at > 28.8 μM. Rank correlation confirmed a significant reduction in the number of long-lived closed events in the range of 0.5–28.8 μM Ca^{2+} from five patches ($R_S = -0.61$; $P < 0.01$; $n = 26$).

Voltage dependence

The voltage dependence of channel activity was investigated at an approximately half maximum as well as at a saturating $[Ca^{2+}]_i$. The membrane potential of nine inside-out membrane patches superfused with 3.6 μM Ca^{2+} ($n = 5$) and with 115 μM Ca^{2+} ($n = 4$) was varied between −40 mV and +40 mV. In each patch 3–10 sets of data were recorded at 3–5 different membrane potentials and P_O and opening frequency were determined. Regression analysis showed that these parameters did not depend on membrane potential ($P = 0.15$–0.96). The relations between membrane potential and P_O and opening frequency of one patch containing at least three channels superfused with 3.6 μM Ca^{2+} are depicted in Figs. 5a and b.

Open time frequency density distributions were con-

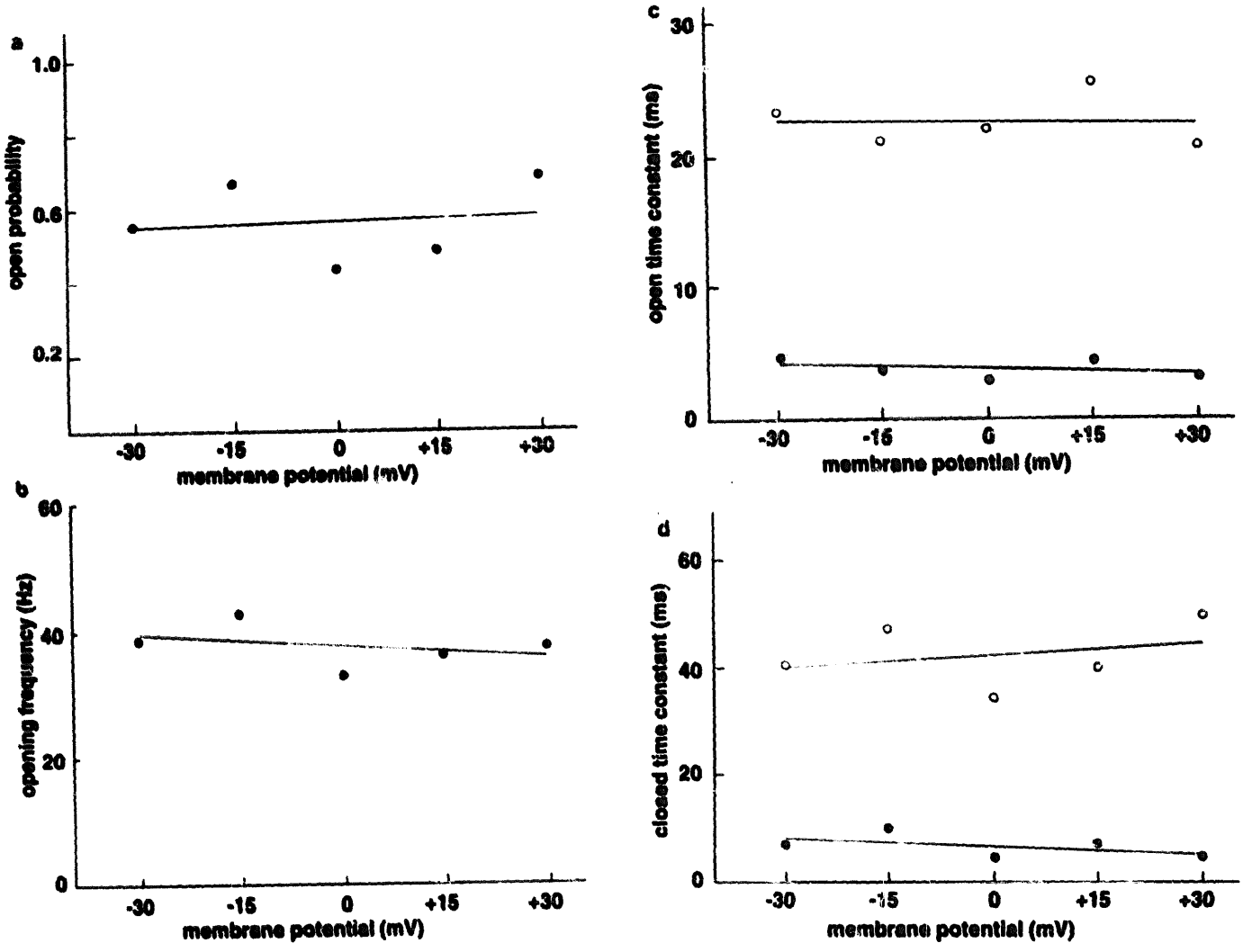

Fig. 5. The absence of an effect of membrane potential on Ca^{2+}-activated K^+ channel activity of human erythrocytes. The open probability (a) and the opening frequency (b) of the inside-out patch ery1152 at 3.6 μM Ca^{2+} show no voltage-dependence (no regression: $P = 0.89$ and 0.46, respectively). The two open time constants (c) and the two closed time constants (d) of the inside-out patch ery1023a at 115 μM Ca^{2+} at various membrane potentials are neither voltage-dependent (no regression: $P = 0.22$–0.93).

structed from the same nine patches. The two time constants were not voltage-dependent ($P = 0.11$–0.93). An example of the voltage-independence of the two open time constants is illustrated in Fig. 5c.

Closed time frequency density distributions of four apparent single channel patches showed that neither the two closed time constants nor the two relative amplitudes were voltage-dependent ($P = 0.07$–0.80). Fig. 5d illustrates the voltage independence of the two closed time constants for the same patch as used in Fig. 5c.

Discussion

Single-channel properties of Ca^{2+}-activated K^+ channels in human erythrocytes have been characterized under conditions mimicking the physiological K^+ gradient. None of the presently studied parameters describing the single channel activity is voltage-dependent consistent with the previous finding on the opening frequency of the CaK channel in human erythrocytes [8]. A decrease in the mean open time with increasing membrane potential between −100 and +75 mV has been obtained in symmetric high K^+ solutions and with 1 mM Mg^{2+} at the internal side of the membrane [9]. Millimolar concentrations of internal Mg^{2+} reduce the open probability of CaK channels in human erythrocytes [11] and cause a flickery, voltage-dependent block of small CaK channels in rat hippocampal neurons [23]. A similar block of erythrocyte CaK channels by Mg^{2+} might explain the previously observed voltage-dependence of the open probability, which was mainly due to a reduced mean open time. In the present study no Mg^{2+} was added to the internal solution.

The present results demonstrate that the increase in open probability (P_O) with $[Ca^{2+}]_i$ is due to a Ca^{2+}-dependent increase in channel opening frequency, while

TABLE II

Parameters of the dual exponential function $A_1 \exp(-t/\tau_1) + A_2 \exp(-t/\tau_2)$ *fitted to the open time frequency density histograms of* Ca^{2+}*-activated* K^+ *channels*

The last column represents the number of histograms obtained in the patch. For each histogram 50–100 s of data were recorded and analyzed.

Patch	τ_1 (ms)	A_1 (%)	τ_2 (ms)	A_2 (%)	n
ery0725	5.6±2.0	57±17	15.0±3.4	43±17	7
ery0918	4.1±0.6	81± 8	11.6±2.6	19± 8	5
ery0921	3.7±0.4	82± 2	12.5±2.2	18± 2	4
ery0925	3.0±1.3	35±11	20.5±9.4	65±11	5
ery1023a	3.6±0.7	17± 5	22.5±1.9	83± 5	5
ery1023b	4.4±1.5	37±21	14.8±2.5	63±21	5
ery1029	5.0±0.9	40±16	14.1±0.7	60±16	3
ery1101a	4.1±1.9	21± 3	37.9±3.9	79± 3	6
ery1101b	10.4±2.9	33±20	34.2±7.3	67±20	4
ery1115ab	5.3±1.7	18± 6	31.6±4.9	82± 6	5
ery1115b	9.5±5.8	36±22	32.0±9.1	64±22	5
ery11152	5.0±3.0	26± 8	17.3±3.9	74± 8	5

the single-channel open times remain constant and only a long-lived closed state is sensitive to $[Ca^{2+}]_i$. This result indicates that the Ca^{2+}-dependent K^+ current in human erythrocytes is regulated by the frequency of channel opening over a wide range of $[Ca^{2+}]_i$. Thus, the Ca^{2+} concentration-dependent operation of CaK channels in human erythrocytes shows analogy to that of acetylcholine-gated ion channels, at which the agonist also enhances the probability that an opening event occurs, but not the characteristics of the open event itself [24,25].

The slope values of the curves relating P_O and channel opening frequency to $[Ca^{2+}]_i$ are not significantly different from 1, which is consistent with the involvement of a single Ca^{2+} ion binding site in CaK channel opening. It has previously been suggested that two Ca^{2+} ions are needed to activate the CaK channel in human erythrocytes [9,10]. However, in these studies $[Ca^{2+}]_i$ was buffered using EGTA, which is a relatively weak buffer for $[Ca^{2+}] \geq 1$ μM. On the other hand citric acid, which is suited to buffer high $[Ca^{2+}]$, is a weak buffer in the low concentration range [22] (see Methods). Therefore, the formerly reported slope factor [9,10] is more likely an overestimate, whereas in the present study the slope factor of the concentration-effect curve may be slightly underestimated. The difference in Ca^{2+} buffer capacity may also account for the difference between the presently observed value of 4.7 μM and the previously reported value of 2 μM for the EC_{50} of the open probability concentration-effect curve [10].

The open time distributions of the CaK channel in human erythrocytes reveal at least two open states. Similarly, the closed time distributions indicate the presence of at least two closed states. The two open and two closed times are independent of $[Ca^{2+}]_i$. However, with increasing $[Ca^{2+}]_i$ the lifetime or the probability of a third, long-lived closed state decreases, as indicated by a marked reduction of the number of records without channel opening. Two open states of CaK channels in human erythrocytes have been reported before and both time constants as well as the relative amplitudes of the two components appeared to depend on temperature [13]. The presently obtained values for the two open time constants are in the same range as those previously reported. The present results contrast with the previous finding that the mean open time of erythrocyte CaK channels depends on Ca^{2+} concentration [9]. This discrepancy cannot be explained at present. The possible blocking effect of millimolar concentrations of internal Mg^{2+}, which might compete with Ca^{2+} has been discussed above. With regard to the Ca^{2+} dependence of the closed times of erythrocyte CaK channels divergent results have been published before [9,11].

The amplitudes of the two kinetic components of the open time histograms varied considerably between patches as can be seen from their standard deviations (see Table II). Apparently the CaK channel may change its mode of opening from predominantly short to predominantly long open times. BK channels from rat skeletal muscle have been reported to exhibit different modes of opening [26]. The presently observed variability is not due to heterogeneity in the Ca^{2+} sensitivity of CaK channels, since channel open lifetimes are independent of $[Ca^{2+}]_i$ and the variation in EC_{50} values is relatively small. In case of heterogeneous populations of CaK channels one would expect to obtain at least some patches with fast or slow channels only. The variability more likely resides in different membrane properties or in some common shared factor interacting with the channel protein. The latter hypothesis is particularly attractive. Molecular biological investigations of voltage-dependent [27,28] and ligand-gated channels [29,30] have revealed subunit structures of channel proteins. K^+ channels are also supposed to possess a multimeric subunit structure [31]. Dynamic assembly and disassembly of such subunits in the patch membrane could account for both the negative cooperativity and the heterogeneity of CaK channels observed. This hypothesis requires further investigation.

The *I–V* relationship revealed a single CaK channel conductance of 15 pS between −40 and +40 mV and showed rectification in the more negative membrane potential range. The conductance of the CaK channel in human erythrocytes measured in symmetric high K^+ solutions is 10–40 pS [8,10]. Under similar asymmetric K^+ conditions as used in the present study a single CaK channel conductance of 14 pS was obtained in Friend murine erythroleukemia cells and the single-

channel conductance increased to 50 pS in high external K^+ solution [32]. The former value is close to the presently obtained unitary conductance of 15 pS. The range of membrane potentials presently investigated is too narrow to make further inferences on rectification.

In non-excitable cells CaK channels are thought to be involved in regulatory cell volume control [33]. It has been suggested that the increase of K^+ permeability caused by the increased $[Ca^{2+}]_i$ in human erythrocytes would also serve the purpose of volume regulation [34]. The present results show that optimum activation of CaK channels in human erythrocytes is attained only at $[Ca^{2+}]_i$ beyond the normal physiological range. This could indicate that with physiological variation of internal Ca^{2+} only few CaK channels activate and a large channel reserve is maintained. Alternatively, the low sensitivity of CaK channels to $[Ca^{2+}]_i$ would be functional when Ca^{2+} influx leads to locally high Ca^{2+} concentrations at the inner face of the membrane before disturbing cellular Ca^{2+} homeostasis. The occurrence of intracellular Ca^{2+} gradients has already been demonstrated by means of Ca^{2+}-sensitive fluorescent dye techniques [35,36].

Acknowledgements

The authors wish to acknowledge Ing. A. de Groot for electronics and computer support as well as R. Zwart and H. Wiesenegger for the majority of blood samples used in this study. This investigation was supported by the Foundation for Biological Research (BION), which is subsidized by the Netherlands Organization for Scientific Research (NWO).

References

1 Gárdos, G. (1958) Biochim. Biophys. Acta 30, 653–654.
2 Simons, T.J.B. (1976) J. Physiol. 256, 227–244.
3 Porzig, H. (1977) J. Membr. Biol. 31, 317–349.
4 Yingst, D.R. and Hoffman, J.F. (1984) J. Gen. Physiol. 83, 19–45.
5 Wolff, D., Cecchi, X., Spalvins, A. and Canessa, M. (1988) J. Membr. Biol. 106, 243–252.
6 Hoffman, J.F. and Blum, R.M. (1977) in Membrane Toxicity (Miller, M.V. and Shammoo, A.E., eds.), pp. 381–405, Plenum Press, New York.
Burgess, G.M., Claret, M. and Jenkinson, D.H. (1984) J. Physiol. 317, 67–90.
8 Hamill, O.P. (1981) J. Physiol. 319, 97P–98P.
9 Grygorczyk, R. and Schwarz, W. (1983) Cell Calcium 4, 499–510.
10 Grygorczyk, R., Schwarz, W. and Passow, H. (1984) Biophys. J. 45, 693–698.
11 Grygorczyk, R. and Schwarz, W. (1985) Eur. Biophys. J. 12, 57–65.
12 Stampe, P. and Vestergaard-Bogind, B. (1989) J. Membr. Biol. 112, 9–14.
13 Grygorczyk, R. (1987) Biochim. Biophys. Acta 902, 159–168.
14 Leinders, T., Van Kleef, R.G.D.M. and Vijverberg, H.P.M. (1992) Pflügers Arch. 420, R38.
15 Hamill, O.P., Marty, A., Neher, E., Sakmann, B. and Sigworth F.J. (1981) Pflügers Arch. 391, 85–100.
16 Bendat, J.S. and Piersol, A.G. (1971) Random data: Analysis and measurement procedures, Wiley-Interscience, New York.
17 Marquardt, D.W. (1963) J. Soc. Indust. Appl. Math. 11, 431–441.
18 Diem, K. and Lentner, C. (1971) Wissenschaftliche Tabellen, pp. 175–180, Ciba-Geigy, Basel.
19 Shields, M., Grygorczyk, K., Fuhrmann, G.F., Schwarz, W. and Passow H. (1985) Biochim. Biophys. Acta 815, 223–232.
20 Oberhauser, A., Alvarez, O. and Latorre, R. (1988) J. Gen. Physiol. 92, 67–86.
21 Van Heeswijk, M.P.E., Geertsen, J.A.M. and Van Os, C.H. (1984) J. Membr. Biol. 79, 19–31.
22 Sillen, L.G. and Martell, A.E. (1971) Stability constants of metal-ion complexes. Suppl. No. 1, Special Publication No. 25, The Chemical Society, London.
23 Lancaster, B., Nicoll, R.A. and Perkel, D.J. (1991) J. Neurosci. 11, 23–30.
24 Sakmann, B., Patlak, J. and Neher, E. (1980) Nature 286, 71–73.
25 Sine, S.M. and Steinbach, J.H. (1986) J. Physiol. 373, 129–162.
26 McManus, O.B. and Magleby, K.L. (1988) J. Physiol. 402, 79–120.
27 Noda, M., Shimizu, S., Tanabe, T., Takai, T., Kayano, T., Ikeda, T., Takahashi, H., Nakayama, Y., Minamino, N., Kangawa, K., Matsuo, H., Raftery M.A., Hirose, T., Inayama, S., Hayashida, H., Miyata, T. and Numa, S. (1984) Nature 312, 121–127.
28 Tanabe, T., Takeshima, H., Mikami, A., Flockerzi, V., Takahashi, H., Kangawa, K., Kojima, M., Matsuo, H., Hirose, T. and Numa, S. (1987) Nature 328, 313–318.
29 Schofield, P.R., Darlison, M.G., Fujita, N., Burt, D.R., Stephenson, F.A., Rodriquez, H., Rhee, L.M., Ramachandran, J., Reale, V., Glencorse, T.A., Seeburg, P.H. and Barnard, E.A. (1987) Nature 328, 221–227.
30 Cooper, E., Couturier, S. and Ballivet, M. (1991) Nature 350, 235–238.
31 Tempel, B.L., Papazian, D.M., Schwarz, T.L., Jan, Y.N. and Jan, L.Y. (1987) Science 237, 770–775.
32 Arcangeli, A., Wanke, E., Olivotto, M., Carnagni, S. and Ferroni, A. (1987) Biochem. Biophys. Res. Commun. 146, 1450–1457.
33 Hoffmann, E.K. and Simonsen, L.O. (1989) Physiol. Rev. 69, 315–381.
34 Halperin, J.A., Brugnara, C. and Nicholson-Weller, A. (1989) J. Clin. Invest. 83, 1166–1171.
35 Gorman, A.L.F., Levy, S., Nasi, E. and Tillotson, D. (1984) J. Physiol. 353, 127–142.
36 Hernandez-Cruz, A., Sala, F. and Adams, P.R. (1990) Science 247, 858–862.